PROCEEDINGS OF SCIENCE

Role of fission in the r-process nucleosynthesis

Aleksandra Kelić [1] **and Karl-Heinz Schmidt**
GSI
Planckstr. 1, D-64291 Darmstadt, Germany
E-mail: a.kelic@gsi.de

Fission can have an important influence on the termination of the r process and on the abundances of long-lived actinides, which are relevant for the determination of the age of the Universe. Fission could also influence the abundances of nuclei in the region A~90 and 130 due to fission cycling. In order to quantitatively understand the fission role in the r process, two important pieces of information are needed: the fission probabilities and mass- and charge-distributions of the fission fragments. Unfortunately, experimental information is only available for nuclei in a limited region of the nuclide chart, and for heavy r-process nuclei one has to rely on theoretical predictions. This manuscript reviews the status of present experimental and theoretical knowledge on some aspects of fission which are important input for the r-process calculations.

.

International Symposium on Nuclear Astrophysics – Nuclei in the Cosmos – IX
CERN, Geneva, Switzerland
25-30 June, 2006

[1] Speaker

PoS(NIC-IX)063

1. Introduction

In order to have a full understanding of the r-process nucleosynthesis it is necessary to have proper knowledge on the fission process. In the r process, fission can have an important influence on the abundances of long-lived actinides, which are relevant for determination of the age of the Galaxy and the Universe [1]. In scenarios where high neutron densities exist over long periods, fission will influence the abundances of nuclei in the region A~90 and ~130 due to the fission cycling [2,3]. In similar scenarios, fission can also have decisive influence on the termination of the r-process and production of super-heavy elements [4].

Studies on the role of fission in the r process began forty years ago [2]. Meanwhile, extensive investigations on beta-delayed, neutron-induced and neutrino-induced fission have been performed; see e.g. [3,5,6,7,8,9,10]. One of the common conclusions from all this work is that the influence of fission on the r process is very sensitive to the fission-barrier heights of heavy r-process nuclei with $A > 190$ and $Z > 84$, since they determine the calculated fission probabilities of these nuclei. Moreover, information on mass- and charge-distributions of fragments formed in the fission of these heavy r-process nuclei is essential if one wants to calculate r-process abundances.

In this contribution, we will concentrate on the status of experimental and theoretical knowledge on fission which is needed as input for r-process calculations. We will discuss in details the heights of fission barriers and the fragment formation in fission. Firstly, using available experimental data on saddle-point and ground-state masses, we will present a detailed study on the predictions of different models concerning the isospin dependence of saddle-point masses [11]. Secondly, we will present a model for calculating mass- and charge-distributions of fission fragments that can correctly predict the transition from double-humped to single-humped distributions with decreasing mass of the fissionning system and increasing excitation energy in the light actinides. Detailed r-process network calculations with fission included are discussed in the contribution by G. Martinez-Pinedo *et al.* to this Proceedings.

2. Fission barriers

One of the most important ingredients for calculating fission probabilities is the height of the fission barrier. Unfortunately, experimental information on fission-barrier heights is only available for nuclei in a limited region of the nuclide chart, as it can be seen in Figure 1. Therefore, for heavy r-process nuclei one has to rely on theoretically calculated barriers. Due to the limited number of available experimental barriers, in any theoretical model, constraints on the parameters defining the dependence of the fission barrier on neutron excess are rather weak. This leads to large uncertainties in estimating the heights of the fission barriers of heavy nuclei involved in the r process. For example, it was shown in Ref. [6] that predictions on the beta-delayed fission probabilities for nuclei in the region $A \sim 250 - 290$ and $Z \sim 92 - 98$ can vary between 0% and 100 % depending on the model used, thus strongly influencing the r-process termination point. Moreover, the uncertainties within the nuclear models used to calculate the fission barriers can have important consequences on the r process. Meyer *et al.* have shown that

a change of 1 MeV in the fission-barrier height can have strong consequences on the production of the progenitors ($A \sim 250$) of the actinide cosmochronometers, and thus on the nuclear cosmochronological age of the Galaxy [12].

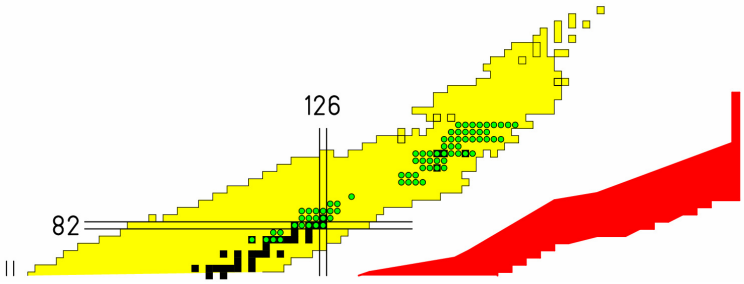

Figure 1 Available data (green dots) on fission barriers for $Z \geq 80$ taken from the RIPL-2 library [13] and shown on the nuclear chart. Black squares represent the stabile nuclei, and the red marked region a possible r-process path.

Recently, important progress has been made, see e.g. [14] in developing full microscopic approaches to nuclear fission. Nevertheless, due to the complexity of the problem, this type of calculations is difficult to apply to heavy nuclei, where one has still to deal with semi-empirical models. Often used models are of the macroscopic-microscopic type, where the macroscopic contribution to the masses is based either on some liquid-drop, droplet or Thomas-Fermi model, while microscopic corrections are calculated separately, mostly using the Strutinsky method [15]. The free parameters of these models are fixed using the nuclear ground-state properties and, in some cases, the height of fission barriers when available. Some examples of such calculations are shown in Figure 2 (upper part), where the fission-barrier heights given by the results of the Howard-Möller fission-barrier calculations [16], the finite-range liquid drop model (FRLDM) [17], the Thomas-Fermi model (TF) [18], and the extended Thomas-Fermi model with Strutinsky integral (ETFSI) [19] are plotted as a function of the mass number for several uranium isotopes (A = 200-305). In case of the FRLDM and the TF model, the calculated ground-state shell corrections of Ref. [20] were added as done in Ref. [21]. In cases where the fission barriers were measured, the experimental values are also shown. From the figure it is clear that as soon as one enters the experimentally unexplored region there is a severe divergence between the predictions of different models. Of course, these differences can be caused by both – macroscopic and microscopic – parts of the models, but in the present work we will discuss only macroscopic models. For this, we have two reasons: Firstly, different models show large discrepancies in the isotopic trend of macroscopic fission barriers[1] as can be seen in the lower part of Figure 2. Secondly, we want to avoid uncertainties and difficulties in calculating the shell corrections at large deformations corresponding to saddle-point configurations.

Recently, we have performed a study on the behaviour of the macroscopic contribution to the fission barriers when extrapolating to very neutron-rich nuclei [22]. This study was based on the approach of Dahlinger *et al.* [23], where the predictions of the theoretical models were

[1] The macroscopic part of the Howard-Möller calculations is based on the droplet model [24].

examined by means of a detailed analysis of the isotopic trends of ground-state and saddle-point masses.

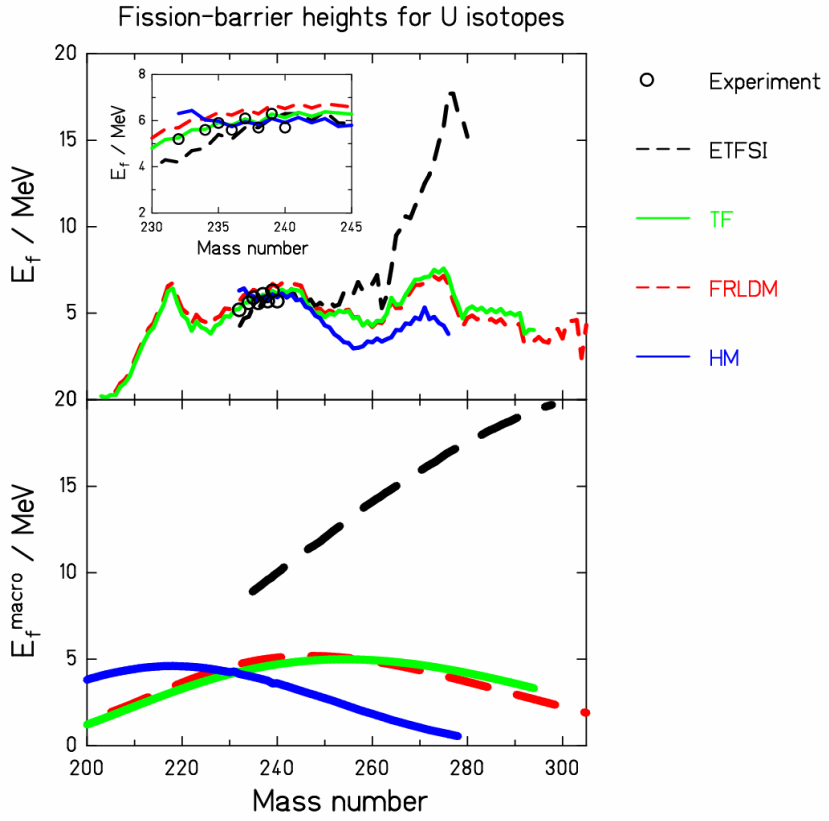

Figure 2 Full macroscopic-microscopic (upper part) and macroscopic part (lower part) of the fission barrier calculated for different uranium isotopes using: the extended Thomas-Fermi model + Strutinsky integral [19] (dashed black line), the Thomas-Fermi model [18] (full green line), the finite-range liquid-drop model [17] (dashed red line), and the Howard-Möller tables [16] (full blue line). In case of FRLDM and TF the ground-state shell corrections were taken from Ref. [20]. The macroscopic part of the Howard-Möller results is based on the droplet model [24]. The small inset in the upper left part represents a zoom of the region where experimental data are available.

In order to test the consistency of these models, we study the difference between the experimental saddle-point mass $M_{sadd}^{\exp}\left(=B_f^{\exp}+M_{GS}^{\exp}\right)$ and the macroscopic part of the saddle-point mass $M_{sadd}^{macro}\left(=B_f^{macro}+M_{GS}^{macro}\right)$ given by the above-mentioned models, with B_f being the height of the fission barrier and M_{GS} the ground-state mass:

$$\delta U_{sad} = M_{sadd}^{\exp} - M_{sadd}^{macro} = (E_f^{\exp} + M_{GS}^{\exp}) - (E_f^{macro} + M_{GS}^{macro}) \quad (1)$$

The difference between experimental and macroscopic mass, δU_{sadd} as given by Eq. 1 should correspond to the empirical shell-correction energy.

What do we know about shell-correction energy at the saddle-point deformation?

It is well known that the shell-correction energy oscillates with deformation and neutron or proton number. If we consider deformations corresponding to the saddle-point configuration,

then the oscillations in the microscopic corrections for heavy-nuclei region we are interested in have a period between about 10 ~ 30 neutrons depending on the single-particle potential used, see e.g. [25,26,27,28]. This means that, if we follow the isotopic trend of the shell-correction energy at the saddle point over a large enough region of neutron numbers, this quantity should show only local variations with the above given periodicity. Moreover, as the shell-correction energy at the saddle point is very small – below 1 – 2 MeV [18,21,29], these local variations should also be very small. In other words, the saddle-point shell-correction energy as a function of neutron number should show only local, periodical, variations with small amplitude; there should be no global tendencies, e.g. increase or decrease with neutron number.

We have used this fact in Ref. [22] to test the macroscopic part of the different, above mentioned, models. Using experimental ground-state masses [30] and experimental fission barriers and different macroscopic models, we have calculated the quantity δU_{sadd} as given by Eq. 1 for a wide range of neutron numbers. If a model describes realistically the isotopic trend, the quantity δU_{sad} will correspond to the shell-correction energy at the saddle point and will fulfil the above-mentioned condition, i.e. the slope of δU_{sad} as a function of neutron number will be close to zero ($\partial(\delta U_{sadd})/\partial N \approx 0$). On the contrary, if a model does not describe realistically the isotopic trend, then the quantity δU_{sad} as a function of neutron number will show global tendencies, like e.g. increase or decrease over a large range of neutron numbers ($\partial(\delta U_{sadd})/\partial N \neq 0$).

For four studied models: the Droplet model [24], the Finite-range liquid drop model [17], the Thomas-Fermi model [18] and the Extended Thomas-Fermi model [19], the slopes ($A_1 = \partial(\delta U_{sadd})/\partial N$) of δU_{sadd} as a function of neutron number are shown in Figure 3 versus atomic number. For more details, see [22].

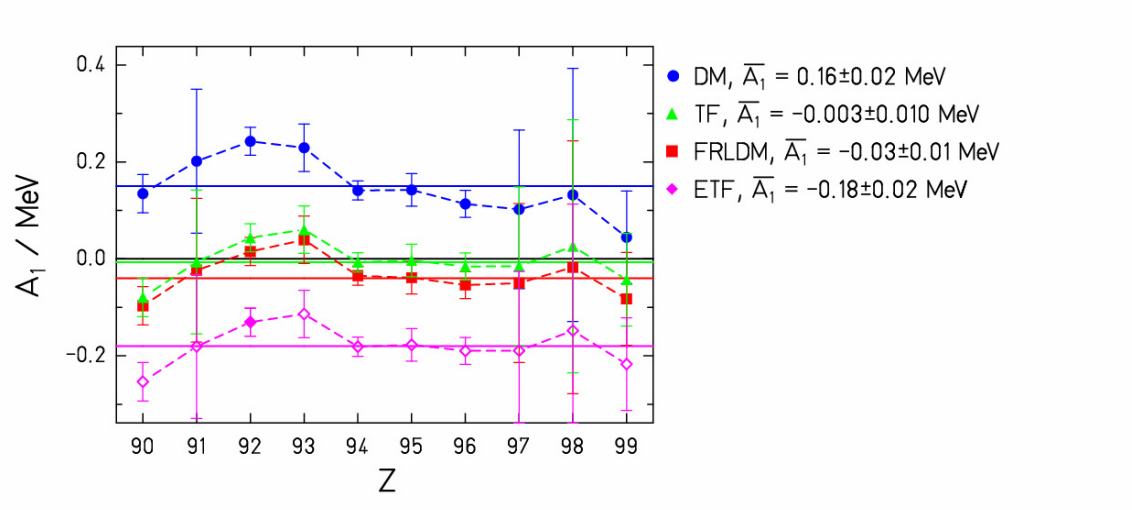

Figure 3 Slopes of δU_{sad} as a function of the neutron excess are shown as a function of the nuclear charge number Z obtained for the droplet model (points), the Thomas-Fermi model (triangles), FRLDM (squares) and the extended Thomas-Fermi model (rhomboids); The full lines indicate the average values of the slopes. The average values are also given in the figure. Error bars originate from the experimental uncertainties in the fission-barrier heights. Dashed lines are drawn to guide the eye. For more details, see [22].

We can see from Figure 3 that the Thomas-Fermi and the Finite-range liquid drop model predict slopes which are very close to zero, while the Droplet and the Extended Thomas-Fermi model result in the slope values which are not consistent with zero.

The results of this study (see also [22]) show that the most realistic predictions are expected from the Thomas-Fermi model [18]. A similar conclusion can be made for the Finite-range liquid-drop model [17] while further improvements in the saddle-point mass predictions of the Droplet model [24] and the Extended Thomas-Fermi model [19] seem to be needed. This result raises doubts on the applicability of the Howard-Möllers fission-barrier tables [16] and the predictions of the ETFSI model [19] in modeling the r-process nucleosynthesis.

3. Mass and charge division in fission

For understanding the role of fission in r-process nucleosynthesis, apart from fission probabilities one also needs masses and atomic numbers of fragments created in fission of heavy progenitors. For example, Qian has recently proposed that the observed structures at $A \sim 90$ and $A \sim 130$ in the r-process abundances in low-metallicity, old galactical halo stars can have their origin in the fission of heavy progenitors $A_{prog} \sim 190 - 320$ [31]. In order to test this and similar other ideas (see e.g [2,3,4,7]) it is needed to determine the mass and charge distributions of the fission fragments formed during the r process.

What is usually assumed in the astrophysical calculations is that either both fission fragments have the same mass and the same atomic number, or that one fragment correspond to the double-magic ^{132}Sn and the second fragment has $A = A_{prog} - 132$ and $Z = Z_{prog} - 50$. Both these assumptions are rather simplistic, and not always supported by the experimental data. This can be clearly seen from Figure 4.

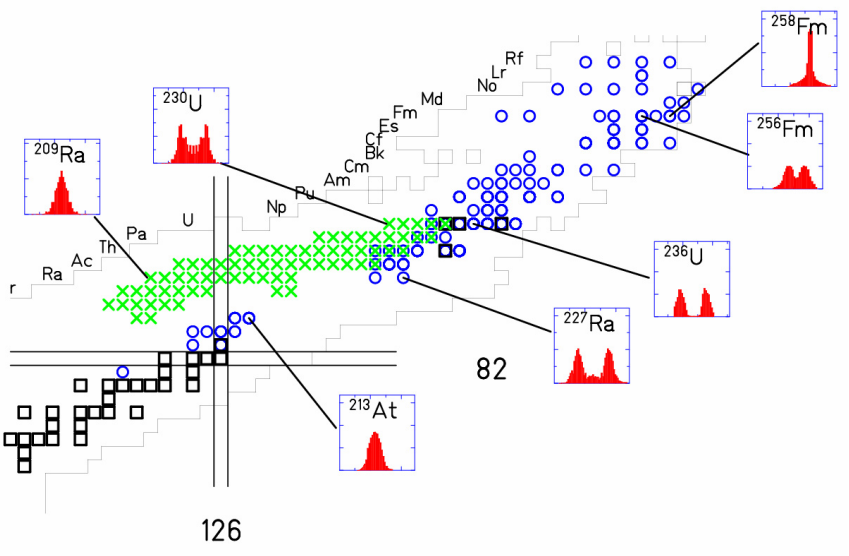

Figure 4 Available experimental data on mass or charge distributions in low-energy fission – green crosses: Z-distributions of fission fragments formed in fission after electro-magnetic excitation [32], blue circles: mass distributions from particle- (mostly neutron-) induced fission. For more details, see Ref. [32]. For several compound nuclei mass or charge distributions of fission fragments are shown in small insets.

For the lightest nuclei shown in Figure 4, the distributions of fission fragments are symmetric. With increasing the mass of the fissionning system we observe a transition to double- and triple-humped distributions, and for the heaviest systems the distributions become again symmetric but with much smaller widths as compared to the lightest systems around astatine. If one looks at fission-fragment distributions for a given isotopic chain of fissionning systems, for nuclei in the actinide region one can see smooth transition from double-, to triple- and then to single-humped distributions for the lightest fissionning systems in the isotopic chain. On the contrary, in case of fermium we see a very abrupt transition from single- to double-humped distribution when going from ^{258}Fm to ^{256}Fm.

In the course of time, different approaches have been developed in order to reproduce and predict mass and charge splits in fission. One can divide them in two groups:

1. Empirical models (e.g. [33,34]) – mass and charge distributions are parametrized using more or less complited mathematical formulas. This kind of approach is very adapted if one is interested in nuclei in regions where experimental data are available, but it is not reliable for extrapolations in unknown regions.
2. Theoretical models – different models have been developed, we list some of them below, together with advanteges and disadvanteges of different models:
    - Strutinsky-type calculations of the potential-energy landscape (e.g. [35]) – Give good qualitative overview on multimodal character of fission, but have no quantitative predictions for fission yields and do not include any dynamics.
    - Statistical scission-point models (e.g. [36,37]) – Give quantitative predictions for fission yields, but do not include any memory on dynamics from saddle to scission.
    - Statistical saddle-point models (e.g. [38]) – Give quantitative predictions for fission yields, but are neglecting dynamics from saddle to scission. Moreover, uncertainty on potential energy leads to large uncertainties in the yields.
    - Time-dependent Hartree-Fock calculations with Generator-coordinate method – Recently, an important progress have been made in full microscopic description of fission including dynamics, see Ref. [39]. Still, no dissipation is included and the approach demands for high computational effort.

In order to surmount these problems, we have developed a model [40] which combines these two approaches. In this semi-empirical approach, the transition from single-humped to double-humped fragment distributions is explained by macroscopic (fissionning nucleus) and microscopic (nascent fragments) properties of the potential-energy landscape near the outer saddle point.

Macroscopic features of the potential-energy landscape are deduced from mass distributions at high excitation energy [41] and Langevin calculations [42], while microscopic features are based on two-centre shell-model calculations [43,44] and theoretical assumptions on washing out of shell effects [45]. The parameters describing the microscopic features in the potential are deduced from data on measured features of fission channels: nuclide yields, neutron yields, *TKE*.

We use certain assumptions on the dynamics of fragment formation, i.e. that the mass division is already determined at the outer saddle point, while the *N/Z* degree of freedom is very

fast compared to the motion from saddle-to-scission and is, therefore, determined at the scission point.

As an example for the application of this approach, we show in Figure 5 a comparison between experimental and model-calculated charge distributions of fragments formed in the electromagnetic-induced fission of several secondary beams ranging from ^{220}Ac to ^{234}U [32]. The transition from single- to triple- and then to double-humped fragments distributions is correctly described by the model. Please note, that all calculations were performed with one and same set of model parameters; no adjustment to individual systems has been done. This global aspect of the approach gives us confidence when extrapolating into regions where no experimental data are available. In case of r-process simulations, the model was applied in refs. [9,10].

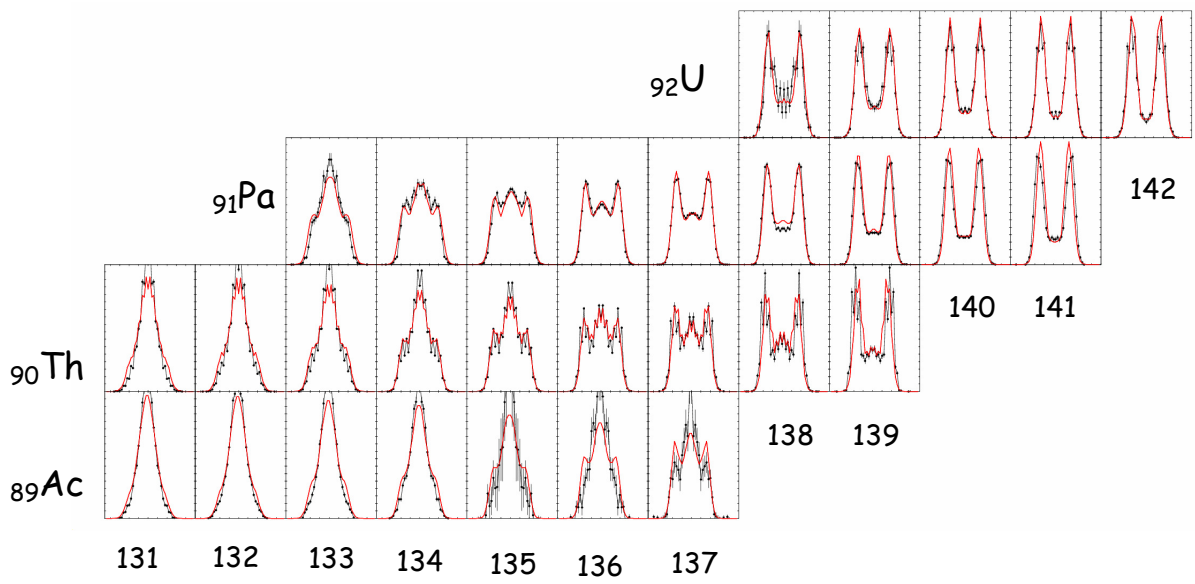

Figure 5 Comparison between measured (black dots) and calculated (red line) fission-fragment nuclear-charge distributions in the range Z = 24 to Z = 65 from ^{220}Ac to ^{234}U in electromagnetic-induced fission shown on a chart of the nuclides. Experimental data are taken from Ref. [32].

4. Conclusions

In this paper we have discussed the status of present experimental and theoretical knowledge on some aspects of fission which are important input for the r-process calculations. We have specifically concentrated on the height of the fission barrier and fragment formation in fission.

Using available experimental data on fission barriers and ground-state masses, we have presented a detailed study of the predictions of different models concerning the isospin dependence of saddle-point masses. Evidence is found that several macroscopic models yield unrealistic saddle-point masses for very neutron-rich nuclei, which are relevant for the r-process nucleosynthesis.

We have also discussed different approaches used to calculate fission-fragment distributions. Empirical systematics are not suited for astrophysical applications. Theoretical approaches still fail to include all important features of the fission process, but they can give good orientation of major trends. A macroscopic-microscopic approach based on macroscopic properties of the fissioning system and microscopic properties of the nascent fission fragments with simplified considerations of dynamical features seems to be a promising tool for robust extrapolations of empirical features**.**

Acknowledgments We are in debt to Karlheinz Langanke, Gabriel Martinez-Pinedo and Nikolaj Zinner for fruitful discussions concerning the r process.

References

[1] J.J. Cowan, F.-K. Thielemann, J.W. Truran, Phys. Rep. 208 (1991) 267.
[2] P.A. Seeger, W.A. Fowler and D.D. Clayton, Astrop. J. 11 Suppl. (1965) S121
[3] T. Rauscher, J.H. Applegate, J.J. Cowan, F.-K. Thielemann, M. Wiescher, Astrop. J. 429 (1994) 49
[4] I. Panov et al., Nucl. Phys. A 747 (2005) 633
[5] F.K. Thielemann, J. Metzinger and H.V. Klapdor-Kleingrothaus, Z. Phys. A 309 (1983) 301
[6] I.V. Panov and F.-K. Thielemann, Astron. Lett. 29 (2003) 510
[7] I.V. Panov, E. Kolbe, B. Pfeiffer, T. Rauscher, K.-L. Kratz and F.-K. Thielemann, Nucl. Phys. A 747 (2005) 633
[8] E. Kolbe, K. Langanke and G.M. Fuller, Phys. Rev. Lett 92 (2004) 111101
[9] A. Kelić, N. Zinner, E. Kolbe, K. Langanke and K.-H. Schmidt, Phys. Lett. B 616 (2005) 48
[10] G. Martinez-Pinedo et al., contribution to this Proceedings
[11] A. Kelić and K.-H. Schmidt, Phys. Lett. B 643 (2006) 362
[12] B.S. Meyer, W.M. Howard, G.J. Mathews, K. Takahashi, P. Möller and G.A. Leander, Phys. Rev. C 39 (1989) 1876
[13] http://www-nds.iaea.org/RIPL-2/
[14] J.M. Pearson and S. Goriely, Nucl. Phys. A in print
[15] V.M. Strutinsky, Nucl. Phys. A 95 (1967) 420
[16] W.M. Howard and P. Möller, At. Data Nucl. Data Tables 25 (1980) 219
[17] A.J. Sierk, Phys. Rev. C 33 (1986) 2039
[18] W.D. Myers and W.J. Swiatecki, Phys. Rev. C 60 (1999) 014606-1
[19] A. Mamdouh, J.M. Pearson, M. Rayet and F. Tondeur, Nucl. Phys. A 679 (2001) 337
[20] P. Möller, J.R. Nix, W.D. Myers and W.J. Swiatecki, At. Data Nucl. Data Tables 59 (1995) 185
[21] W.D. Myers and W.J. Swiatecki, Nucl. Phys. A 601 (1996) 141
[22] A. Kelić and K.-H. Schmidt, Phys. Lett. B 642 (2006) 362
[23] M. Dahlinger, D. Vermeulen and K.-H. Schmidt, Nucl. Phys. A 376 (1982) 94
[24] W.D. Myers, „Droplet Model of Atomic Nuclei“, 1977 IFI/Plenum, ISBN 0-306-65170-X
[25 D. Scharnweber, U. Mosel and W. Greiner, Phys. Rev. Lett. 24 (1970) 601
[26] M. Bolsterli, E.O. Fiset, J.R. Nix and J.L. Norton, Phys. Rev. C 5 (1972) 1050
[27] P. Möller and J.R. Nix, „Physics and Chemistry of Fission“, Proceedings of a conference at Rochester (IAEA, Vienna 1974), Volume 1, page103.
[28] J. Randrup, S.E. Larson, P. Möller, S.G Nilsson, K. Pomorski, A. Sobiczewski, Phys. Rev. C 13 (1976) 229
[29] K. Siwek-Wilczyńska, I. Skwira, and J. Wilczyński , Phys. Rev. C 72, 034605 (2005)
[30] G. Audi, A. H. Wapstra and C. Thibault, Nucl. Phys. A 729 (2003) 337

[31] Y.-Z. Qian, Astr. J. 569 (2002) L103
[32] K.-H. Schmidt et al., Nucl. Phys. A 665 (2000) 221
[33] F. Atchison, Proceedings of a Specialists Meeting Issy-Les-Moulineaux, France (1994), p. 199.
[34] V. Rubchenya et al., Nucl. Instrum. Methods A 463 (2001) 653
[35] P. Möller, D. G. Madland, A. J. Sierk and A. Iwamoto, Nature 409 (2001) 785
[*36*] P. Fong, Phys. Rev. C 17 (1978) 1731
[37] B. D. Wilkins, E. P. Steinberg and R. R. Chasman, Phys. Rev. C 14 (1976) 1832
[38] M. C. Duijvestijn, A. J. Koning and F.-J. Hambsch, Phys. Rev. C 64 (2001) 014607
[39] H. Goutte et al., Phys. Rev. C 71 (2005) 024316
[40] J. Benlliure, A. Grewe, M. de Jong, K.-H. Schmidt and S. Zhdanov, Nucl. Phys. A 628 (1998) 458
[41] Ya. Rusanov et al., Phys. At. Nucl. 60 (1997) 683
[42] P. N. Nadtochy, G. D. Adeev and A. V. Karpov, Phys. Rev. C 65 (2002) 064615
[43] J. Maruhn and W. Greiner, Z. Phys. 251 (1972) 431
[44] V. V. Pashkevich, Nucl. Phys. A 477 (1988) 1
[45] A. V. Ignatyuk, G. N. Smirenkin and A. S. Tiskin, Yad. Fiz. 21 (1975) 485 (Sov. J. Nucl. Phys. 21 (1975) 255)